

Published in final edited form as:

Rep U S. 2012 October 12; 2012: 1982–1987. doi:10.1109/IROS.2012.6385535.

## A Hand-held Instrument for in vivo Probe-based Confocal Laser Endomicroscopy during Minimally Invasive Surgery

**Win Tun Latt [Member, IEEE],**

Singapore Polytechnic, Singapore. Phone: + 65 (0) 9169 4230; Fax: +65 (0) 6772 1975.  
win\_tun\_latt@sp.edu.sgrobotics.researcher@gmail.com

**Tou Pin Chang,**

Department of Surgery & Cancer, Imperial College London, UK. t.chang@imperial.ac.uk

**Aimee Di Marco,**

Department of Surgery & Cancer, Imperial College London, UK

**Philip Pratt,**

Hamlyn Centre for Robotic Surgery, Imperial College London, UK

**Ka-Wai Kwok,**

Hamlyn Centre for Robotic Surgery, Imperial College London, UK

**James Clark, and**

Department of Surgery & Cancer, Imperial College London, UK

**Guang-Zhong Yang [Fellow, IEEE]**

Hamlyn Centre for Robotic Surgery, Imperial College London, UK

### Abstract

Probe-based confocal laser endomicroscopy (pCLE) provides high resolution imaging of tissue in vivo. Maintaining a steady contact between target tissue and pCLE probe tip is important for image consistency. In this paper, a new prototype hand-held instrument for in vivo pCLE during Minimally Invasive Surgery (MIS) is presented. The proposed instrument incorporates adaptive force sensing and actuation, allowing improved image consistency and force control, thus minimizing tissue deformation and induced micro-structural variations. The performance and accuracy of the contact force control are evaluated in detailed laboratory settings and in vivo validation of the device during transanal microsurgery in a live porcine model further demonstrates the potential clinical value of the device.

### Keywords

hand-held imaging probe; force adaptive control; confocal endomicroscopy; pCLE; tissue characterization; TEM; TEO

### I. Introduction

Development of smart surgical instruments integrated with miniaturized imaging probes for in situ, in vivo imaging has been increasingly in demand following recent advances in

biophotonics. ‘Optical biopsy’ methods, such as optical coherence tomography [1][2] and confocal endomicroscopy [3][4] have been gaining popularity due to their ability to provide high resolution in vivo tissue images which have the potential to enhance diagnosis, and provide valuable real-time information during endoscopic procedures or open surgery. The examination of various sites such as gastrointestinal tract lumen [5], lung [6], bladder [7], and peritoneal cavity [8] can feasibly be performed using a probe-based confocal laser endomicroscopic system (pCLE). In such a system, the probe ( $\varnothing < 2.5\text{mm}$ ) is passed either through the working channel of an endoscope, or laparoscopic port. The integration of pCLE into such diagnostic procedures confers benefits, as discussed previously [9].

Manipulation of the pCLE probe, however, plays a crucial part in obtaining consistency with such highly magnified images. The probe tip requires steady contact with the tissue, regardless of movement of the operator, bowel mobility, peristalsis and cardiorespiratory movement. Small variations in contact force demonstrably alter the image and the information acquired, especially at low-magnitude contact forces. The effect of contact force between pCLE probe tip and colonic tissue is to alter crypt morphology [10]. A ‘compression effect’ is seen in pCLE of the peripheral lung [11], and pressure effects have been shown in probe-based spectroscopic methods [12].

There are two main approaches that can facilitate steady tissue contact with the probe tip, hence obtaining consistent images: passive force control, and active force control. The passive force control approach [13] can maintain steady tissue contact regardless of tissue motion by pushing the probe hard against the tissue with high-magnitude force, which must be more than a few hundred millinewtons. Variation in the contact force due to tissue motion does not alter steadiness of the tissue contact as long as the magnitude of the contact force remains above a few hundred millinewtons. Active force control, as the name implies, can maintain steadiness of the tissue contact by actively controlling the contact force to remain at the desired force magnitude. The later is preferred over the former for the following reasons: 1) it allows low-magnitude contact force which facilitates sliding the probe over the tissue for mosaicing of the tissue images [14], 2) it permits the magnification of tissue structures to be varied as the operator desires (for example, by keeping magnitude of the contact force low, the number of colonic crypts that can be seen in an image can be increased without mosaicing of images [14]), and 3) it prevents inadvertent exertion of large forces that can damage or perforate the tissue.

Various force control systems or devices have been developed for different medical applications. To aid in peeling of skin grafts, Duchemin *et al.* [15][16] developed a robotic system for maintaining a desired contact force. Force control for grasping soft tissue is presented in [17]. To assist in a mitral valve repair procedure, a force control hand-held instrument was designed and developed [18]. To make minute forces big enough to be felt by the hand in micromanipulation, hand-held force magnifying devices have been developed [19][20]. Although these systems can control contact force, they are not designed for use with pCLE probes.

A force control system using a robotic endoscope to maintain constant contact force between the tissue and the pCLE probe is described in [21][22]. The probe runs through the operating

channel of the endoscope and the contact force at the distal tip is inferred from a force/torque sensor mounted at the proximal- end of the probe. Since the system is designed for use with a robotic endoscope, it is impractical for use during open surgery or when evaluating ex vivo tissue samples.

To provide surgeons with a versatile platform for pCLE examination in cases that do not require minimally invasive access, a hand-held instrument [9] was previously created which compensates for contact force variations owing to tissue motion and erroneous or involuntary motion of the hand. To enhance acquisition of consistent pCLE images in minimally invasive surgery while maintaining simplicity and facilitating versatile use in evaluation of ex-vivo tissue samples, a new hand-held instrument is designed and developed. Example applications in which the new instrument can be used include transanal endoscopic microsurgery [23], and laparoscopic surgery.

## II. Methods

### A. Actuator Selection

Since the instrument is designed to be hand-held, the actuator needs be small, lightweight, and sufficiently fast to compensate for the disturbance force due to tissue motion as well as erroneous motion of the operator's hand. Erroneous motion of the hand has three main components: physiological tremor [24], jerk [25], and drift [26]. The frequency band of physiological tremor for a well-supported hand is 8 to 12Hz.

It has been discussed in our previous study [9] that the effect of physiological tremor on image consistency is negligible due to the relatively small amplitude of motion. Jerk is a higher frequency component that occurs rarely. Drift is a low frequency component (mostly less than 3Hz), and its amplitude can be a few hundred microns when the arm is well-supported [27] and can reach a few millimeters if it is not well-supported.

To compensate for tissue motion, the actuator must have sufficient stroke length to cover the range of motion of the tissue, and be sufficiently fast for its bandwidth. Breathing and cardiac beating cause significant range of motion of tissue. Average liver tissue movement due to breathing is reported to be approximately 10mm [28], while the range of motion of the mitral valve of a heart is approximately 20mm [1].

Therefore, the bandwidth of the actuator should be higher than 3 Hz while its stroke length should be approximately 20 mm. Finally, to ensure versatility across different clinical scenarios, the actuator should be sufficiently strong in order to provide up to a few Newtons of force. Based on the above specifications, a linear DC-servomotor (LM 1247-020-01, Faulhaber, Germany) is chosen in preference to other types of actuators for its compactness, rapid response, adequacy of stroke length and force.

### B. Instrument Design

The instrument consists of a linear three-phase DC-servomotor integrated with analog Hall Sensors (LM 1247-020-01, Faulhaber, Germany), a force sensor (8438 5005, Burster), and a 2.5mm diameter pCLE probe (Cellvizio Coloflex UHD, Mauna Kea Technologies, Paris,

France). Figure 1 shows the instrument and its scale in comparison to an operator's hand. The proximal-end unit consisting of the force sensor and the linear motor measures approximately  $\text{Ø}32 \times 100$  mm. The whole instrument measures 350 mm in length, and 150 grams in weight. The instrument body and the connecting parts such as the heads of the out- and inner-shaft, are fabricated with Vero black material using a rapid prototyping machine (Objet EDEN350™, Objet Geometries Ltd., USA). The instrument handle is made of aluminum while the inner-shaft is a brass tube (OD 4mm, ID 3.2mm). The linear DC-servomotor employed can provide a total stroke length of 20 mm and continuous force of 3.6 N. It measures approximately  $12.5 \times 12.5 \times 50$  mm, and weighs 57 grams including the actuator shaft.

Unlike its predecessor [9], the force sensor in this instrument is placed at the proximal-side of the instrument. The force sensor employed can measure up to 5N of force. Forces at the tip of the probe are transmitted to the sensing area of the force sensor courtesy of a set screw that grips the pCLE probe to the inner-shaft that is attached to the force sensor via a screw and a linkage (Figure 2). The force sensor is fixed at the distal-end of the motor shaft. The pCLE probe has a  $\text{Ø}2$ mm cable and  $\text{Ø}2.5$ mm head. However, the design allows other sizes of pCLE probes to be readily used. The force sensor output is amplified using an instrumentation amplifier. The amplifier output is then fed into an analogue input module of a CompactRIO real-time motion controller (CRIO-9114, National Instruments Corp., USA). Root mean square (RMS) sensing noise at the input of the controller is approximately 1.5 mN. The outer-shaft features two linear plastic bearings (ASM-0407-6, Igus® Inc) with outer and inner diameters of 7mm and 4mm, respectively, to provide guidance for the inner-shaft motion, thereby reducing friction. The diameter of the outer-shaft is 9mm, which is small enough to be inserted into most operative ports.

### C. Closed-loop Force Control

For the proposed device, a block diagram of the force feedback closed-loop system is shown in Figure 3.

The contact force  $F_c$  between the tissue and the probe tip is measured by the force sensor. The measured force is acquired through the analog input module (NI 9205 – 16-Bit, 250kS/s) by the CompactRIO real-time controller. The error between the measured force and the desired force  $F_d$  is then used as an input to the PID control scheme implemented in the CompactRIO real-time controller. This generates a voltage (V) through the analog output module (NI 9264, National Instruments Corp.) to the Faulhaber motion controller (MCLM 3006S, Faulhaber). The Faulhaber motion controller, which also employs a PID control scheme, in turn generates motion of the motor shaft by supplying appropriate voltage to the three-phase windings of the motor, based on the analog voltage level received at its input. The loop update rate of the Faulhaber motion controller is set at 0.1 ms while the CompactRIO real-time controller update rate is set at 1 ms.

### III. Experiments and Results

#### A. Bench Tests

Since the force sensor is placed inside the proximal-end unit of the instrument, the force measured by the sensor is the combination of the tissue contact force and the friction between the bearings and the inner-shaft. Consequently, accurate real-time estimation of the friction force and tissue motion is required for accurate control of the contact force.

To evaluate force control performance of the instrument, detailed laboratory evaluation was conducted. As shown in Figure 4, the instrument was clamped at the handle with a vice on the table, and positioned in such a way that perpendicular contact force between the pCLE probe tip and the simulated soft tissue can be measured by a piezoresistive force sensor (FSS1500NS, Honeywell). The piezoresistive sensor was also attached at the end of the shaft of a linear motor (LM0830-015-01, Faulhaber), which provided simulated tissue motion due to respiration. Situated between the force sensor and pCLE probe, a piece of foam was used as the simulated soft tissue. RMS sensing noise of the piezoresistive force sensor is approximately 1 mN.

Magnitudes of the desired tip contact force were varied step-by-step from 0 to 800 mN with 100 mN of increment after each step. The simulated tissue was made stationary while desired contact forces were varied. The desired tip contact force, the force measured by the force sensor at the proximal-end, and the measured tip contact force are shown in Figure 5.

Force control performance was tested where the desired tip contact force is sinusoidal with a peak-to-peak magnitude of 800 mN at 0.2 Hz. Results are shown in Figure 6. The maximum error of the tip contact force is approximately 120mN without friction compensation. This is reduced by about 50% to 60mN peak with friction compensation, performed by adding or subtracting a pre-determined friction force to or from the desired force, and subsequently using the resultant desired force as the input to the controller. Addition or subtraction was performed in the knowledge of the force trajectory.

#### B. An Ex vivo Test with Porcine Bowel Tissue

Prior to in vivo animal experimentation, a simulated in vivo environment was created using porcine bowel tissue, as shown in Figure 7. The instrument was inserted through one of the two holes inside the trocar, and clamped so that the pCLE probe pointed at the desired tissue location. As shown in Figure 8, the force levels were varied step-by-step. The error between measured force at the proximal-end sensor and the desired tip contact force is approximately 4mN RMS.

#### C. In vivo Porcine Experiment

A live porcine trial was conducted under ethical approval (80/2297) to evaluate the potential clinical performance of the instrument. The instrument was evaluated in the context of transanal endoscopic microsurgery, a minimally invasive technique for the local resection of rectal tumours. In vivo examination of the rectum was performed using pCLE.

The trocar (#24941 TK, Karl Storz GmbH, Germany) was inserted transanally. The standard trocar cap was replaced with a customized cap consisting of an elastic sealing diaphragm that accommodates two holes for insertion of the endoscope and instrument integrated with the pCLE probe. The purpose of the diaphragm is to maintain effective pneumorectum. The modified trocar has an outer diameter of 40 mm and a working length of 75 mm. The instrument integrated with the pCLE probe was inserted through one of the two holes in the diaphragm while the endoscope (Ø5 mm) was inserted through the other hole. Pneumorectum was maintained throughout.

In the first step, the instrument's handle was clamped to the operating table with a Martins Arm in such a manner that the pCLE probe tip pointed at the desired tissue location in the porcine rectum. Desired contact force levels were set at 50 mN, 150 mN, 300 mN, 500mN, and 1000 mN, with each level lasting approximately 30 s. In the second step, the instrument's handle was held by hand. Contact force control was performed with the same set of desired contact force levels. The pCLE images acquired at 12Hz during the contact force level of 1000 mN are shown in Figure 10.

#### IV. Discussion

The pCLE probe in its current form is highly flexible and therefore, from the outside, it is difficult to position its tip at an arbitrary desired tissue location inside the body without an internally aided structure. The objective of the instrument design is not only to provide steady contact between the probe tip and the tissue in minimally invasive procedures but also to aid the positioning of the pCLE probe tip inside the body cavity so that it can acquire images from tissue locations that are accessible through manipulation in linear direction.

Although the instrument was evaluated in a transanal endoscopic microsurgery set-up, it can readily be used in other minimally invasive procedures such as laparoscopic surgery and in the examination of tissues inside the peritoneal cavity, as the external diameter of the instrument's outer-shaft is smaller than the internal diameter of most laparoscopic ports.

Compared to the robotic endoscope [22], the instrument described in this paper is simpler, less expensive, and inherently more accurate in force sensing. This is due to the fact that the instrument shaft is straight. The limitation of the instrument in its current form is its inability to direct the probe tip to rectal mucosa where curved access is required. However, in the transanal endoscopic microsurgery set-up, the system is capable of positioning the tip of the pCLE probe on all four quadrants of the visible rectal mucosa wall.

Examining Figure 5 and Figure 8, performance of force control based on the proximal-end force sensor was deemed to be satisfactory. However, due to friction between the inner-shaft and the bearings, the contact force at the tip could not be estimated precisely and therefore its control might not be as accurate as desired. As demonstrated in Figure 5 and Figure 6, the magnitude of force of error is within the range of a few hundreds millinewtons. It is therefore difficult to maintain steady tissue contact at low-magnitude contact force. Incidentally, movements of the proximal end of the pCLE probe affected the accuracy of contact force sensing.

Despite tissue motion due to deformation in pneumorectum, the instrument was able to maintain steady tissue contact at high-magnitude forces and we were able to obtain consistent images when the contact force was set at 1N (Figure 11). However, the image consistency was affected at low-magnitude contact forces and therefore in its current form, the instrument might not be suitable to facilitate fine movements of the probe tip for the purposes of constructing 'mosaics' for a larger field of view.

During this in vivo study, the absence of a rectosigmoid junction in the porcine model caused difficulties in maintaining consistent pneumorectum pressures. As a result, the rectal tissue was inadequately distended and was relatively flaccid in comparison to the equivalent human setting. This caused inadvertent contact with the rectal mucosa, and therefore reduced the accuracy of pCLE probe tip contact force sensing. The lack of an adequate consistent endoscopic view, along with the floppiness of the rectal mucosal wall, might have resulted in the inner shaft head coming in contact with the rectal wall instead of the pCLE probe tip. This might explain the deterioration of images despite high contact force levels.

In summary, this novel hand-held instrument provided the operator with the ability to maintain steady tissue contact at high-magnitude contact forces, and due to the rigidity of the shaft guiding the probe, to position the probe at desired tissue locations. Furthermore, the unique force-sensing properties exhibited by the instrument might help prevent the exertion of excessive contact forces, which otherwise could potentially damage or perforate the tissue.

## V. Conclusion

A prototype hand-held instrument to aid in the acquisition of consistent pCLE images in MIS has been designed and developed. Future work includes improvement of the instrument design to overcome the discovered issues. By replacing some parts made from the Vero black material with metal, further instrument robustness will be achieved.

## Acknowledgments

We gratefully acknowledge financial support from the Wellcome Trust and the assistance of Northwick Park Institute for Medical Research (NPIMR) for trial arrangement.

## References

- [1]. Huang D, et al. Optical coherence tomography. *Science*. 1991; 254(5035):1178–1181. [PubMed: 1957169]
- [2]. Cahill RA, et al. Intraperitoneal virtual biopsy by fibered optical coherence tomography (OCT) at natural orifice transluminal endoscopic surgery (NOTES). *J. Gastrointest Surg.* 14:732–8. [PubMed: 19997982]
- [3]. Kiesslich R, et al. In Vivo Histology of Barrett's Esophagus and Associated Neoplasia by Confocal Laser Endomicroscopy. *Clinical Gastroenterology and Hepatology*. 2006; 4(8):979–987. [PubMed: 16843068]
- [4]. Wallace MB, Fockens P. Probe-based confocal laser endomicroscopy. *Gastroenterology*. 2009; 136:1509–13. [PubMed: 19328799]
- [5]. Pohl H, et al. Miniprobe confocal laser microscopy for the detection of invisible neoplasia in patients with Barrett's oesophagus. *Gut*. 2008; 57:1648–53. [PubMed: 18755886]

- [6]. Thiberville L, Moreno-Swirc S, Vercauteren T, Peltier E, Cave C, Bourg Heckly G. In vivo imaging of the bronchial wall microstructure using fibered confocal fluorescence microscopy. *Am J Respir Crit Care Med.* 2007; 175:22–31. [PubMed: 17023733]
- [7]. Sonn GA, Jones SN, Tarin TV, Du CB, Mach KE, Jensen KC, et al. Optical biopsy of human bladder neoplasia with in vivo confocal laser endomicroscopy. *J Urol.* 2009; 182:1299–305. [PubMed: 19683270]
- [8]. von Delius S, et al. Transgastric in vivo histology in the peritoneal cavity using miniprobe-based confocal fluorescence microscopy in an acute porcine model. *Endoscopy.* 2007; 39:407–11. [PubMed: 17516346]
- [9]. Latt WT, et al. A Hand-held Instrument to Maintain Steady Tissue Contact during Probe-Based Confocal Laser Endomicroscopy. *IEEE Trans Biomed Eng.* Sep; 2011 58(9):2694–2703. [PubMed: 21768038]
- [10]. Newton RC, Noonan DP, Payne C, Andreyev J, Di Marco A, Scarzanella MV, Darzi A, Yang G-Z. Probe tip contact force and bowel distension affect crypt morphology during confocal endomicroscopy. *Gut.* 2011; 60:A12–A13.
- [11]. Thiberville L, et al. Human in vivo fluorescence microimaging of the alveolar ducts and sacs during bronchoscopy. *Eur Respir J.* 2009; 33:974–85. [PubMed: 19213792]
- [12]. Ti Y, Lin WC. Effects of probe contact pressure on in vivo optical spectroscopy. *Opt Express.* 2008; 16:4250–62. [PubMed: 18542520]
- [13]. Rosa, B.; Herman, B.; Szewczyk, J.; Gayet, B.; Morel, G. Laparoscopic optical biopsies: In vivo robotized mosaicing with probe-based confocal endomicroscopy; *IEEE/RSJ International Conference on Intelligent Robots and Systems; CA, USA.* Sep. 2011;
- [14]. Becker V, Vercauteren T, von Weyhern CH, Prinz C, Schmid RM, Meining A. High-resolution miniprobe-based confocal microscopy in combination with video mosaicing (with video). *Gastrointestinal Endoscopy.* 2007; 66:1001–7. [PubMed: 17767932]
- [15]. Duchemin, G.; Dombre, E.; Pierrot, F.; Poignet, P. Robotized Skin Harvesting; 8th Int. Symp. on Exp. Robotics; 8-11 July 2002; Italy.
- [16]. Duchemin, G.; Dombre, E.; Pierrot, F.; Poignet, P. *Experimental Robotics VIII. Vol. 5.* Springer Verlag; Berlin, Germany: 2003. p. 404-413.
- [17]. Stoll, J.; Dupont, P. Force control for grasping soft tissue; *IEEE Int. Conf. on Robotics and Automation; May 2006; Orlando, Florida.*
- [18]. Yuen SG, et al. Force tracking with feed-forward motion estimation for beating heart surgery. *IEEE Trans. on Robotics.* Oct.2010 26(5)
- [19]. Stetten G, Wu B, Klatzky R, Galeotti J, Siegel M, Lee R, Mah F, Eller A, Schuman J, Hollis R. Hand-held force magnifier for surgical instruments. *Proc. Information Processing in Computer-Assisted Interventions.* 2011; 6689:90–100. *Lecture Notes in Computer Science*
- [20]. Payne, CJ.; Latt, WT.; Yang, G-Z. A New Hand-Held Force-Amplifying Device for Micromanipulation; *IEEE International Conference on Robotics and Automation; 2012.* p. 1583-1588.
- [21]. Noonan, DP.; Payne, CJ.; Shang, J.; Newton, R.; Darzi, A.; G.-Z, Yang. Maintaining Constant Tissue Contact Force for an Imaging Probe during Confocal Laser Endomicroscopy; *Hamlyn Sym. on Medical Robotics; 25 May; The Royal Society, London UK.*
- [22]. Noonan, DP.; Payne, CJ.; Shang, J.; Sauvage, V.; Newton, R.; Elson, D.; Darzi, A.; Yang, G-Z. Force adaptive multi-spectral imaging with an articulated robotic endoscope; *MACCAI 2010, MICCAI 2010, Part III; 2010.* p. 245-252. *Lecture Notes in Computer Science*
- [23]. de Graaf EJR, Doornebosch PG, Stassen LPS, Debets JMH, Tetteroo GWM, Hop WCJ. Transanal endoscopic microsurgery for rectal cancer. *European Journal of Cancer.* 2002; 38:904–910. [PubMed: 11978515]
- [24]. Harwell RC, Ferguson RL. Physiologic tremor and microsurgery. *Microsurgery.* 1983; 4:187–192. [PubMed: 6669016]
- [25]. Schenker, PS., et al. Development of a telemanipulator for dexterity enhanced microsurgery; *Proc. 2nd Int. Symp. Med. Rob. Comput. Assist. Surg.; 1995.*
- [26]. Hotraphinyo, LF.; Riviere, CN. Precision Measurement for Microsurgical Instrument Evaluation; *Proc. of the 23rd Annu. EMBS International Conference; Istanbul, Turkey. 2001;*

- [27]. HotrAPHInyo, LF.; Riviere, CN. Three-dimensional accuracy assessment of eye surgeons. Proc. 23rd Annu. Conf. IEEE Eng. Med. Biol. Soc.; Istanbul. 2001;
- [28]. Balter JM, Dawson LA, Kazanjian S, McGinn C, Brock KK, Lawrence T, Haken RT. Determination of ventilatory liver movement via radiographic evaluation of diaphragm position. Int J Radiat Oncol Biol Phys. 2001; 51(1):267–270. [PubMed: 11516877]
- [29]. Yuen SG, Kettler DT, Novotny PM, Plowes RD, Howe RD. Robotic motion compensation for beating heart intracardiac surgery. Int. J. of Robotics Research. 2009; 28(10):1355–1372.

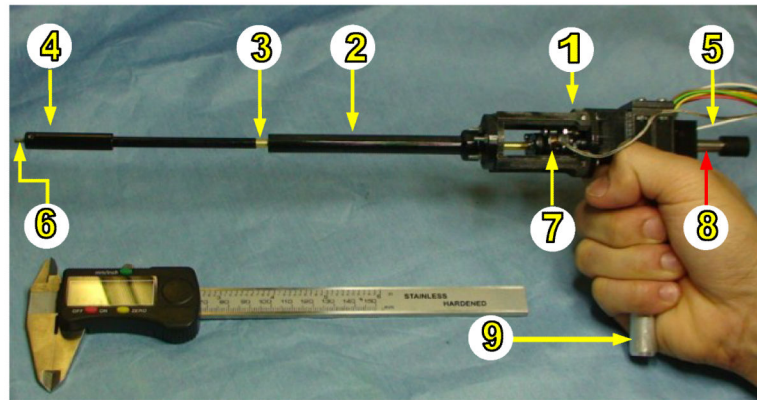


**Figure 1.** The hand-held instrument showing proximal-end unit (1), the outer-shaft (2), the inner-shaft (3), the inner-shaft head (4), the pCLE probe (5), the pCLE probe tip (6), the force sensor (7), the motor shaft (8), and the instrument handle (9).

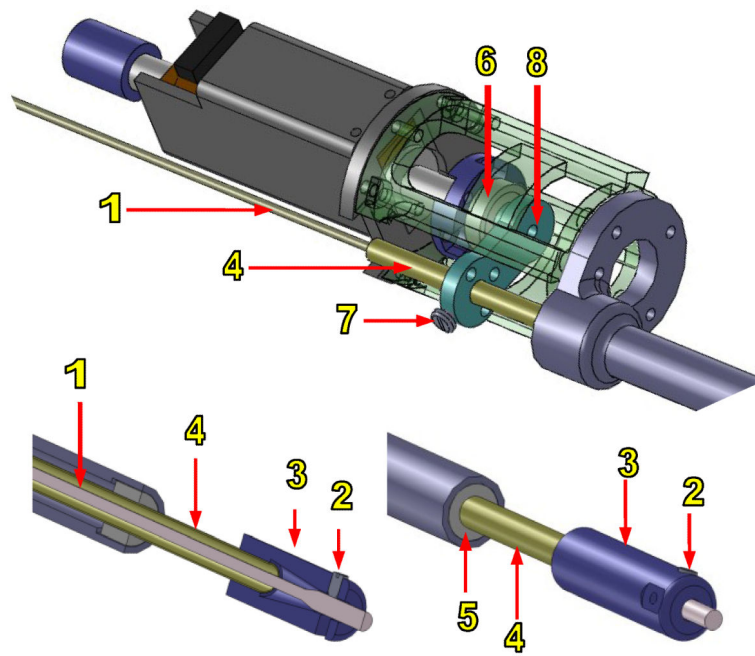


**Figure 2.**

A CAD drawing of the instrument without the handle. The pCLE probe (1) is gripped by a set screw (2) to the inner-shaft head (3), which is tightly fitted to the inner-shaft (4). The inner-shaft supported by bearings (5) is then connected to the force sensor (6) by means of a screw (7) and a linkage (8).

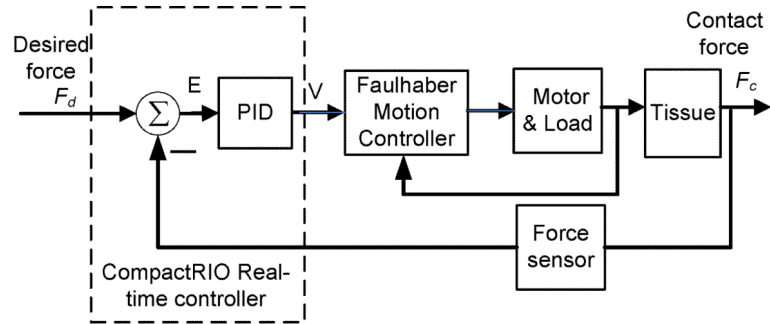


**Figure 3.**

An overview of the closed-loop force control system. The symbol ' $F_c$ ' represents the contact force while the symbol ' $F_d$ ' the desired force.

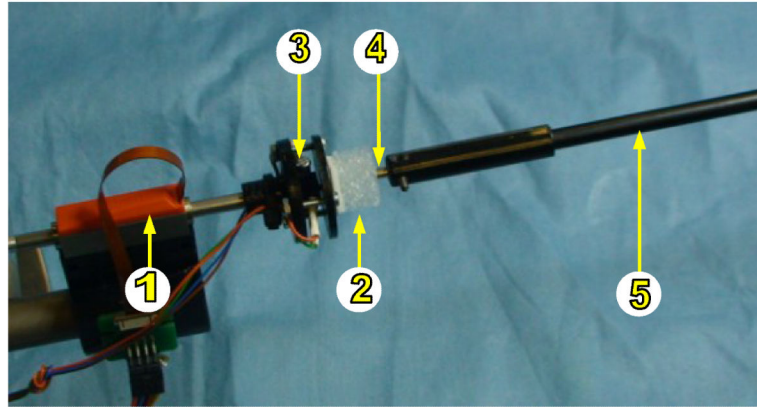


**Figure 4.** Bench test set up showing the linear actuator (1) for motion of simulated tissue (2), and the piezoresistive force sensor (3) to measure the tip contact force, the pCLE probe tip (4), and the inner-shaft (5) of the instrument.

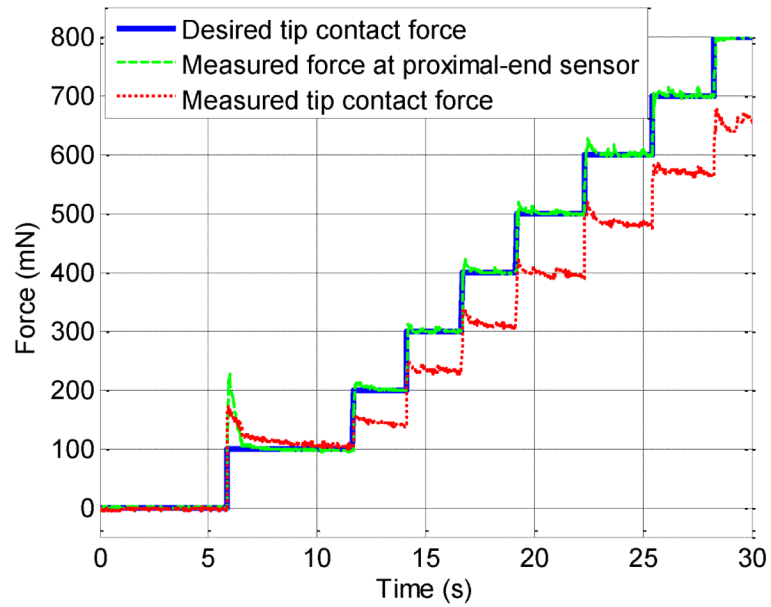


**Figure 5.** Comparison of the contact force at the tip of the instrument and the force measured at the proximal-end force sensor. The force at the tip was measured with the piezoresistive force sensor.

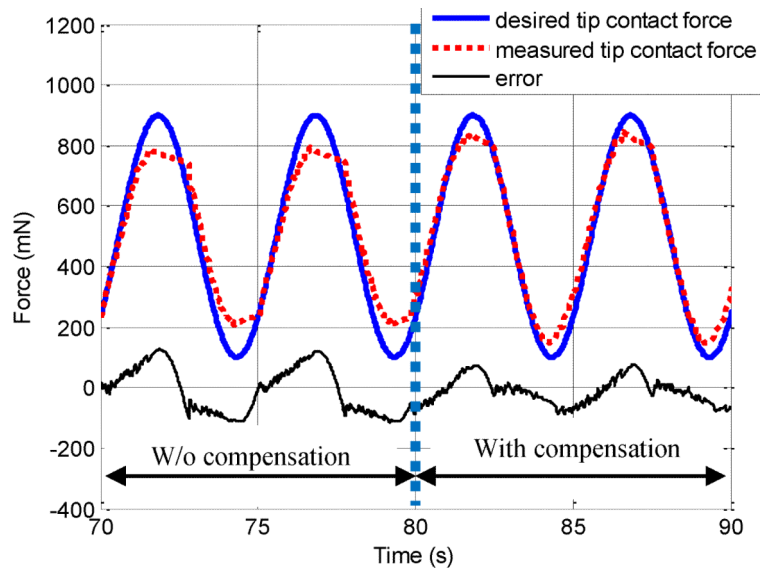


**Figure 6.** Tip contact force error reduction with friction compensation. The plots on the right of the vertical-dotted line are with friction compensation, while those on the left are without.

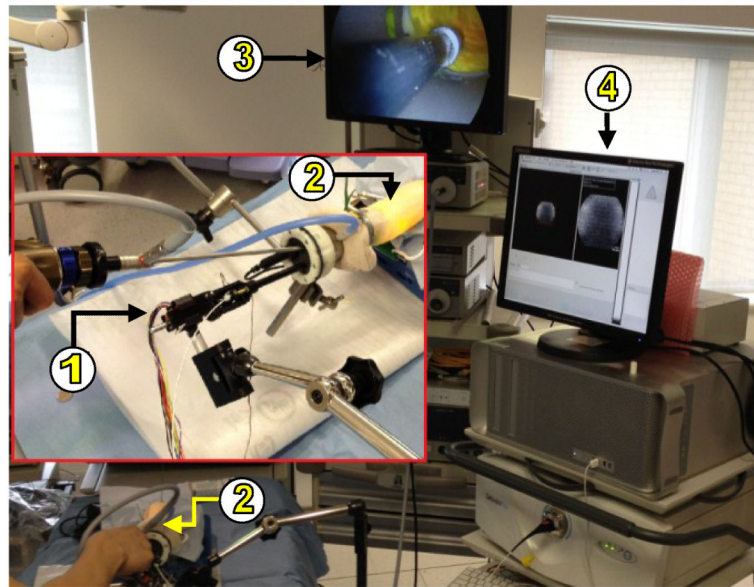


**Figure 7.** Setup for the ex vivo test showing the instrument (1), the bowel tissue (2), endoscopic video display (3), and pCLE video display (4).

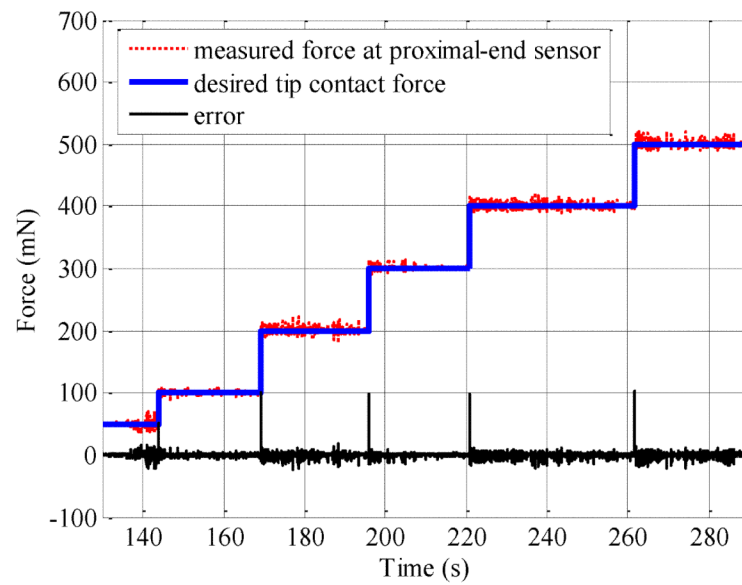


**Figure 8.** Comparison of desired tip contact force, force measured by the proximal-end force sensor, and the error between the desired force and the measured force. The transient spikes are due to the transition of the current desired force level to the next higher level.

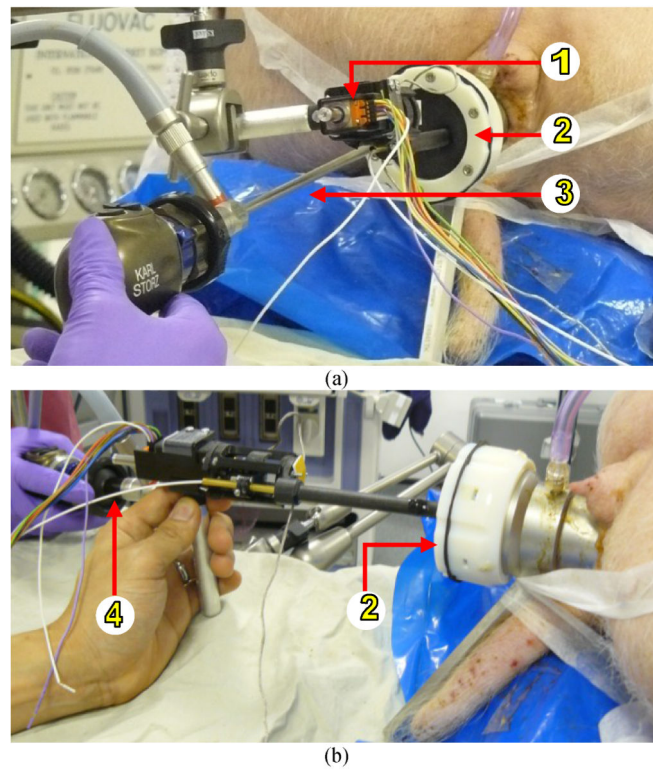


**Figure 9.** Acquisition of pCLE images in the porcine trial using the instrument which was clamped (a), and handheld (b). The instrument (1), the trocar (2), the instrument for endoscopic camera (3), and the pCLE probe (4) are identified.

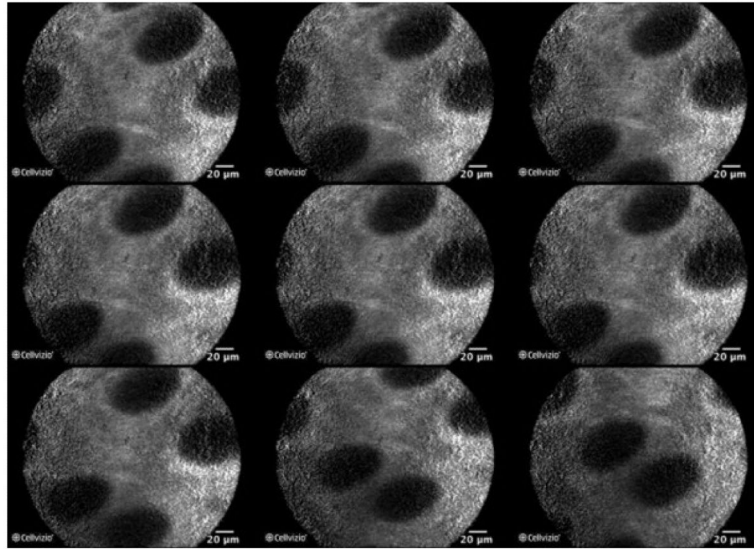


**Figure 10.**  
Consecutive images acquired from the rectal mucosa when the desired contact force was set at 1N.

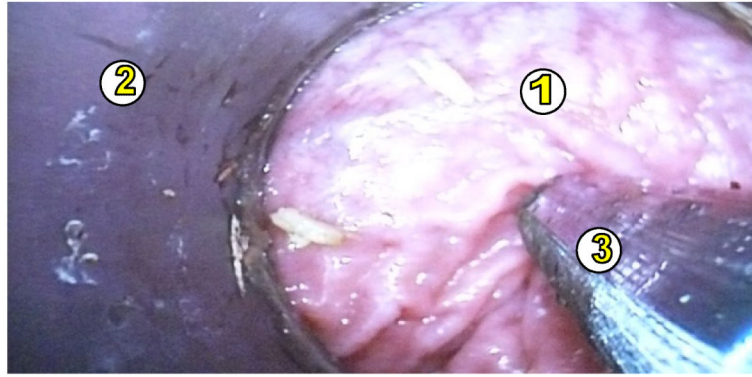


**Figure 11.**  
An endoscopic camera view of the rectum tissue (1), inner wall of the trocar (2), and the instrument's inner-shaft head (3).